Received: 30 August 2020 | Revised: 3 December 2020 | Accepted: 14 December 2020

DOI: 10.1002/aoc.6151

FULL PAPER

Applied Organometallic Chemistry WILEY

Immobilized some of vanadium compounds on modified graphene oxide as nanofiber network for epoxidation of allyl alcohols

Faezeh Farzaneh | **Zahra Ahmadi** | **Zahra Azarkamanzad** | **Maryam Ghahremani**

Department of Chemistry, Faculty of Physics & Chemistry, Alzahra University, Tehran, Iran

Correspondence
Faezeh Farzaneh, Department of Chemistry, Faculty of Physics & Chemistry, Alzahra University, P.O. Box: 1993891176, Vanak, Tehran, Iran.
Email: farzaneh@alzahra.ac.ir; faezeh_farzaneh@yahoo.com

$VO(acac)_2$ and the in situ generated VO(Salen) complex were immobilized on the covalently modified graphene oxide (GO) with ethylenediamine (en) and designated as $VO(acac)_2$@en-GO and VO@Salen@en-GO, respectively. Characterization of the prepared compounds was carried out with FT-IR, XRD, ICP, CHN, Raman, SEM, TEM, and BET techniques. The SEM results confirmed the formation a nanofiber network and nanointerconnected needles. The prepared immobilized complexes were then used as heterogeneous catalysts for epoxidation of some allyl alcohols such as geraniol, *trans*-2-hexene-1-ol, and 1-octen-3-ol. Based on the results obtained by GC and GC–mass analyses, epoxidation of geraniol with 97% conversion and 100% selectivity seemed promising. Readily recycling of the catalyst and reusing for four successive catalytic runs without significant loss of activity revealed that this catalysis system deserves nomination for practical application.

KEYWORDS

allyl alcohols, epoxidation, modified graphene oxide, Schiff base complex, vanadylacetylacetonate

1 | INTRODUCTION

To date, the application of heterogenized homogeneous catalysts is interested due to economical and environmental reasons. In fact, immobilization of metal complexes with covalent binding on different supports through ligand spacer is a common method.[1–3] A wide range of matrixes has been developed for covalent attachments such as inorganic mesoporous,[4,5] or microporous materials,[6] metal–organic frameworks,[7,8] and modified magnetic nanoparticles.[9,10] Recently, two-dimensional supports such as graphite and graphite oxide with unique properties[11–13] have emerged as ideal supports for a variety of catalytic species.[14–17] Besides the availability of surface functionalization, their two-dimensional structures allow excellent dispersion of the catalytic species. Reactive species can readily access the active sites with limited mass transfer resistance. Therefore, remarkable catalytic performance of graphene oxide (GO) as supported catalysts has been observed owing to the presence of plenty of hydroxyl, epoxy, carboxyl, and carbonyl groups. Oxygen functionality modifications can establish as active site for anchoring ions and complexes.[18–22] Therefore, it has been recognized as an ideal candidate for supporting various transition metal complexes.[2] Modification of GO by some reagents such as three methoxysilane (TMS) and ethylenediamine has been extensively investigated.[23–26] In recent years, remarkable catalytic reactions have been carried out using GO or modified GO as supports for reactions such as Suzuki–Miyaura coupling reaction,[14] decomposition of phenol,[16] photodegradation,[27] immobilization of

https://doi.org/10.1002/aoc.6151

enzymes as catalyst for many organic reactions,[19] and epoxidation of some alkenes.[23,28,29] Epoxides are starting materials for the synthesis of commercial products. Some transition metal compounds with their redox properties such as Ti, Fe, Co, Mn, Mo, Cr, and V are known as active catalysts for epoxidation-type reactions. Among these metals, vanadium compounds have attracted increasing attention due to the redox activity and biological properties. Also, vanadium with multiple oxidation state acts as a Lewis acid in oxovanadium(IV) compounds due to low radius to charge ratio and with high affinity for oxygen transformation reactions. The biomimetic roles of vanadium compounds in biochemical process such as phosphorylation, insulin mimicking, nitrogen fixation, and Haloperoxidation are interesting subject for studying.[30–33]

In this study, the vanadium compounds were immobilized on the modified GO and used as heterogeneous catalyst for epoxidation of some allyl alcohols.

2 | EXPRIMENTAL

2.1 | Materials and instrumentation

All chemicals were purchased from Merck Chemical Company and used without further purification. XRD patterns of powdered samples were carried out on STOE-STADI diffractometer using Cu Kα radiation ($k = 1.5406$ Å) in the 2θ range of 10–60° with accelerating voltage and current of 40 kV and 40 mA, respectively. Scanning electron microscopy (SEM) images were obtained on a Philips XL-30ESEM equipped with an X-ray energy dispersive detector. Transmission electron microscopy (TEM) images were also obtained on Zeiss EM10C-100 KV model. N_2 adsorption–desorption isotherms were measured with a MicrotracBEL BELSORP mini system at liquid N_2 temperature. Before measurements, the sample was outgassed at 120°C for 6 h. The surface area was calculated using the Barrett–Emmett–Teller (BET) method. FT-IR spectra were recorded on a Bruker instrument using KBr pellet technique in the range of 4000–400 cm^{-1}. Raman spectra were obtained using a microspectrometer (Takram P50C0R10) at the laser wavenumber of 631 nm between 400 and 1800 cm^{-1} (dry powder samples). The products were analyzed by gas chromatography (GC) (Agilent Technologies, 6890 Series GC System, HP-5 Phenyl Methyl Siloxane Capillary, 30 m × 530 μm × 1.5 μm Nominal, Carrier Gas; He). GC–MS analyses were performed using an 5973 Network Mass Selective Detector, 6890 Network, GC System, Column; HP Phenyl Methyl Siloxane Capillary, 30 m × 530 μm × 1.5 μm Nominal, Carrier Gas; He. Chemical analyses were performed with Varian 150AX inductively coupled plasma optical emission spectrometer (ICPOES). Elemental analyses were performed on a Heraeus CHN Rapid elemental analyzer.

2.2 | Synthesis of GO

GO was prepared by the modified Hummers' method.[34] Briefly, graphite powder (2 g) and sodium nitrate (1 g) were dissolved in sulfuric acid (45 mL) and stirred vigorously for half an hour in an ice bath. Then, potassium permanganate (5 g) was added to the mixture below 20°C. The mixture which turned from dark black to green was kept stirring for half an hour. The ice bath was then removed, and stirring continued at 35–40°C for another 1 h. Water (45 mL) was then slowly added, and the temperature raised to 98°C and allowed to stand for 40 min with vigorous agitation. Finally, water (200 mL) and H_2O_2 (30%, 6 mL) were added, and the mixture centrifuged and washed with distilled water for 10 times and then dialyzed to obtain the pure GO powder.[35,36] Found %C 52.32, %H 2.2%.

2.3 | Reduction and surface modification of GO: Synthesis of modified GO

In a typical experiment and based on the previously reported procedure,[37] ethylenediamine ($NH_2(CH_2)_2NH_2$) (en) (600 mg) was dissolved in ethanol (35 mL) and added dropwise to a suspension of GO (200 mg) in water (33 mL) under vigorous stirring. The reaction continued for 24 h at room temperature. The resulting mixture was isolated by centrifugation and thoroughly washed with a 1:1 ethanol/water mixture followed by drying in a vacuum oven at 80°C for 12 h prior to characterization. Found %C 57.53, %N 5.95, %H 2.8.

2.4 | Preparation [VO(acac)$_2$]

The oxovanadium complex [VO(acac)$_2$] was prepared based on the previously reported procedure.[38] A mixture of V_2O_5 (5 g), distilled water (15 mL), concentrated sulfuric acid (9 mL), and ethanol (25 mL) was boiled with stirring for 30 min. After filtration, freshly distilled acetylacetone (13 mL) was added to the filtrate followed by slow addition of sodium carbonate (20 g of Na_2CO_3 in 125 mL of water). Recrystallization of the obtained solid from chloroform finally afforded the [VO(acac)$_2$] as blue crystals.

2.5 | Immobilization of $VO(acac)_2$ on modified GO: Synthesis of $VO(acac)_2$@en-GO

Modified GO (0.2 g in 15-mL ethanol) was stirred for 10 min (Solution 1). Subsequently, $VO(acac)_2$ (0.2 g) in distilled water (10 mL) (Solution 2) was slowly added to Solution 1 while stirring, and the mixture heated at reflux for 24 h. After filtering the mixture, the obtained solid was washed with ethanol and dried at 70°C in an oven. Vanadium content was found to be 14.82%.

2.6 | Preparation of Sal@en-GO

Salicylaldehyde (10 mmol, 1.22 g) in ethanol (35 mL) was slowly added to a suspension of en-GO (0.2 g) in water (33 mL), and the mixture was heated at reflux for 24 h. The obtained solid product was separated and washed with ethanol for three times and dried in an oven at 70°C for 24 h.

2.7 | Preparation of VO@Sal@en-GO

Sal@en-GO (0.2 g) in ethanol (15 mL) (Solution 1) was added to $VOSO_4$ (0.2 g) in water (10 mL) (Solution 2) and stirred for 24 h. The obtained solid was washed with ethanol for three times and then dried in an oven at 70°C for 24 h. Vanadium content was found to be 15.76%.

2.8 | General procedure for epoxidation of some allyl alcohols

The catalytic activity of $VO(acac)_2$@en-GO was investigated in the epoxidation of geraniol (or other allyl alcohols) in acetonitrile. Typically, the desired amount of

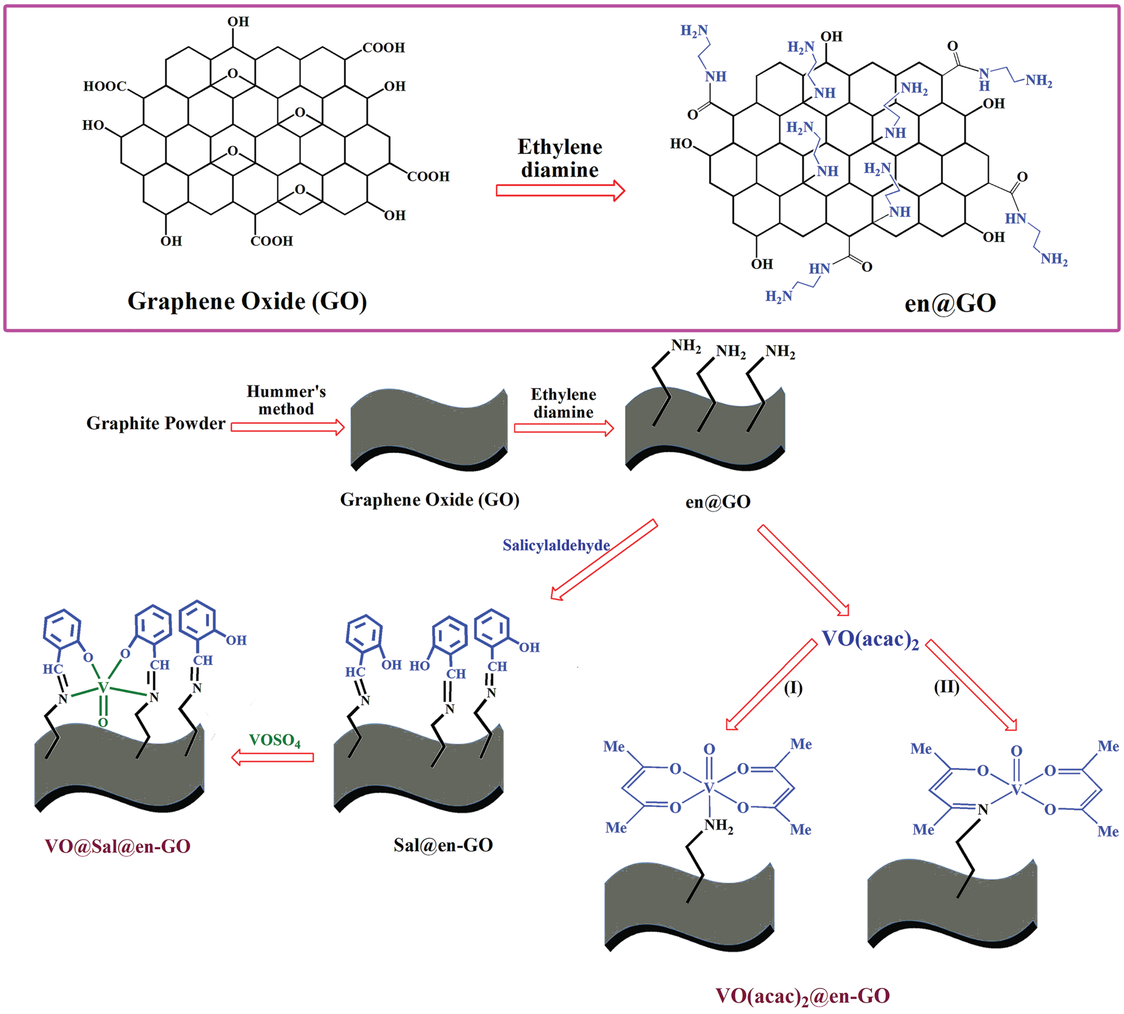

FIGURE 1 Immobilized vanadium compounds on en-GO

catalyst, substrate (10 mmol), and TBHP (12 mmol) in acetonitrile (5 mL) was heated at reflux for the desired time. Upon completion, the catalyst was separated by centrifugation, washed with ethanol, and dried at 100°C. The filtrate was then subjected to GC and GC–mass analysis for identification of products.

3 | RESULTS AND DISCUSSION

As presented in Figure 1, GO was initially prepared by Hummers' method[34] and modified with ethylenediamine (en).[37] VO(acac)$_2$ and the in situ generated VO(Salen) were subsequently immobilized onto the modified GO and designated as VO(acac)$_2$@ en-GO and VO@Sal@en-GO, respectively.

3.1 | Characterization of VO(acac)$_2$@en-GO and VO@Sal@en-GO by FT-IR

The FT-IR spectra of GO, en-GO, and VO(acac)$_2$@en-GO, Sal@en-GO, and VO@Sal@en-GO are shown in Figure 2a–e, respectively. Observation of a peak at 3419 cm^{-1} is due to the O–H stretching vibration of GO (Figure 2a). Additional peaks observed at 2922 and 2853 cm^{-1} are attributed to the C–H stretching vibrations. Observation of peaks at 1704, 1625, and 1384 cm^{-1} are due to the carboxyl C=O, aromatic C=C, and carboxyl O–H groups, respectively.[39] Whereas the peak displayed at 1222 cm^{-1} is attributed to the C–OH stretching vibrations,[40] the other observed at 1052 cm^{-1} is due to the epoxide C–O group.[39] Modification of GO with en (Figure 2b) results in the appearance of two new peaks centered at 3446 and 1560 cm^{-1} due to N–H and C–N stretchings[37] together with a decrease in the intensities of the peaks at 1222 cm^{-1} and 1052 due to the epoxy and alkoxy groups perhaps due to the nucleophilic substitution of $-NH_2$ to the epoxide carbon and the β-carbon of –OH groups. Therefore, the removal of oxygen functionalities from the surface of GO as well as the formation of amine-functionalized graphene is concluded.[37] Finally, the presence of a peak at 970 cm^{-1} as seen in Figure 2c[41,42] due to the V=O vibration confirms the immobilization of vanadium salt onto the modified GO.

FT-IR spectra of Sal@en-GO and VO@Sal@en-GO are shown in Figure 2d,e, respectively. The vibration of C=N in Sal@en-GO appearing at 1645 cm^{-1} (Figure 2d) shifted to a lower frequency after coordination to the VO^{2+} ions (Figure 2e).[28] Moreover, observation of another peak at 976 cm^{-1} was attributed to the V=O stretching vibrations (Figure 2e).[41,42]

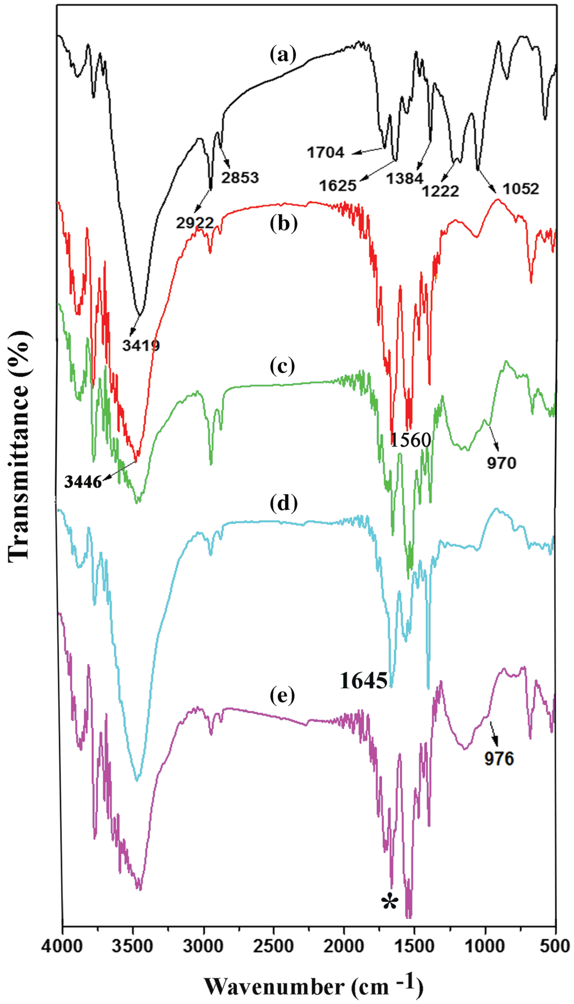

FIGURE 2 FT-IR spectra of (a) GO, (b) en-GO, (c) VO(acac)$_2$@en-GO, (d) Sal@en-GO, and (e) VO@Sal@en-GO

3.2 | XRD of VO(acac)$_2$@en-GOand VO@Sal@en-GO

The XRD patterns of GO, en-GO, VO(acac)$_2$@en-GO, Sal@en-GO, and VO@Sal@en-GO are shown in Figure 3a–e, respectively. The XRD pattern of GO (Figure 3a) shows a peak at $2\theta = 11.1°$ due to the oxygenic functional groups and trapped water molecules between the graphite layers.[43] Compared with the pure GO (Figure 3b), the 001 reflection peak shifted in en-GO perhaps due to the grafting of ethylenediamine into the GO layers.[37]

After immobilization of VO(acac)$_2$ complex onto the en-GO surface, the diffraction peak observed at 11.1° is shifted to 10°, consistent with those reported previously.[43] Moreover, the XRD pattern of VO(acac)$_2$@en-GO shows a broad peak at $2\theta = 26.09°$ (Figure 3c), confirming that the major oxygen-containing groups of GO have been successfully functionalized.[23] The

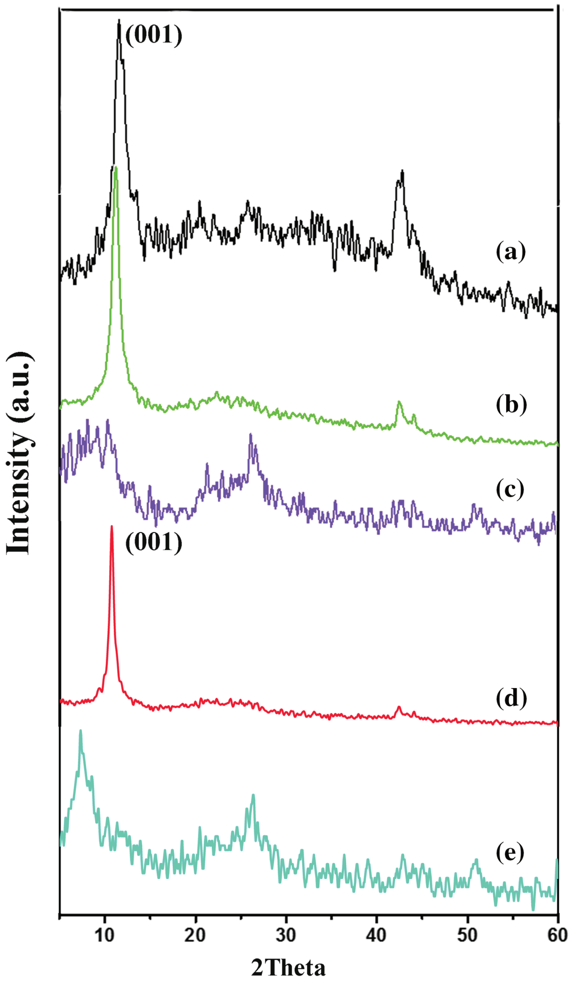

FIGURE 3 The XRD patterns of (a) GO, (b) en-GO, (c) VO(acac)$_2$@en-GO, (d) Sal@en-GO, and (e) VO@Sal@en-GO

XRD patterns of Sal@en-GO and VO@Sal@en-GO shown in Figure 3d–e indicate their similar XRD patterns. After formation of VO@Sal@en-GO, the peak observed nearly at $2\theta = 11.1°$ is shifted and appears as a broader peak at $2\theta = 10°$, consistent with those reported before.[43]

3.3 | Raman spectra of VO(acac)$_2$@en-GO and VO@Sal@en-GO

Recall that the Raman spectroscopy is very sensitive to the electronic structure of carbon-based materials. The Raman spectra of en-GO, VO(acac)$_2$@en-GO, Sal@en-GO, and VO@Sal@en-GO are shown in Figure 4a–d. Raman spectra of GO are characterized by two main peaks generally observed at 1575 and 1349 cm^{-1} which are due to the *sp*^{2}- and *sp*^{3}-hybridized carbon atoms in GO.[37] After functionalization with en, the intensity of these two peaks reduced and shifted to 1560 and 1300 cm^{-1}, respectively. The shifting in GO occurs due to the functionalization of GO with en (Figure 4a). The obtained results are consistent with those reported before.[37,44,45] Particularly significant is observation of a peak at 970 cm^{-1} after immobilization of VO(acac)$_2$ due to the VO stretching vibration (Figure 4b). The other notable point is the decrease in I_D/I_G of GO from 0.97 to 0.94, due to functionalization of GO with en.[37] On the other hand, formation of Sal@en-GO and the position of two peaks due to the en-GO did not changed (Figure 4c). After immobilization of VOSO$_4$ on Sal@en-GO due to the formation of VO@Sal@en-GO, very small peak due to the VO is observed in which its intensity is very low (Figure 4d).

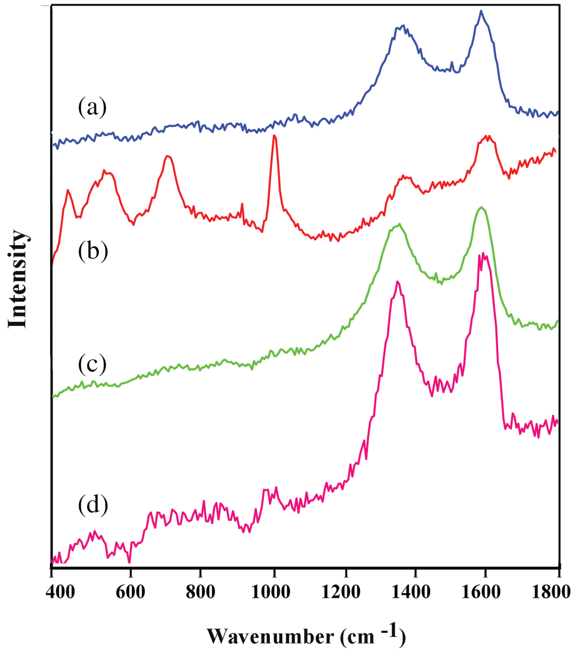

FIGURE 4 Raman spectra of (a) en-GO, (b) VO(acac)$_2$@en-GO, (c) Sal@en-GO, and (d) VO@Sal@en-GO

The SEM images of GO, VO(acac)$_2$@en-GO, and VO@Sal@en-GO are shown in Figure 5a–c, respectively. Based on the SEM images, the formation of nanofiber network and nanointerconnected needles after immobilization of vanadium compounds onto the en-GO is confirmed.

The TEM images of VO(acac)$_2$@en-GO and VO@Sal@en-GO are also shown in Figure 6a–c with two magnifications, respectively. Nanofiber network and nanointerconnected needles are observed.

The nitrogen adsorption–desorption isotherms of GO, en-GO, VO(acac)$_2$@en-GO, and VO@Sal@en-GO are shown in Figure 7 and Table S2. As seen in this figure, the abovementioned materials indicate the Type IV

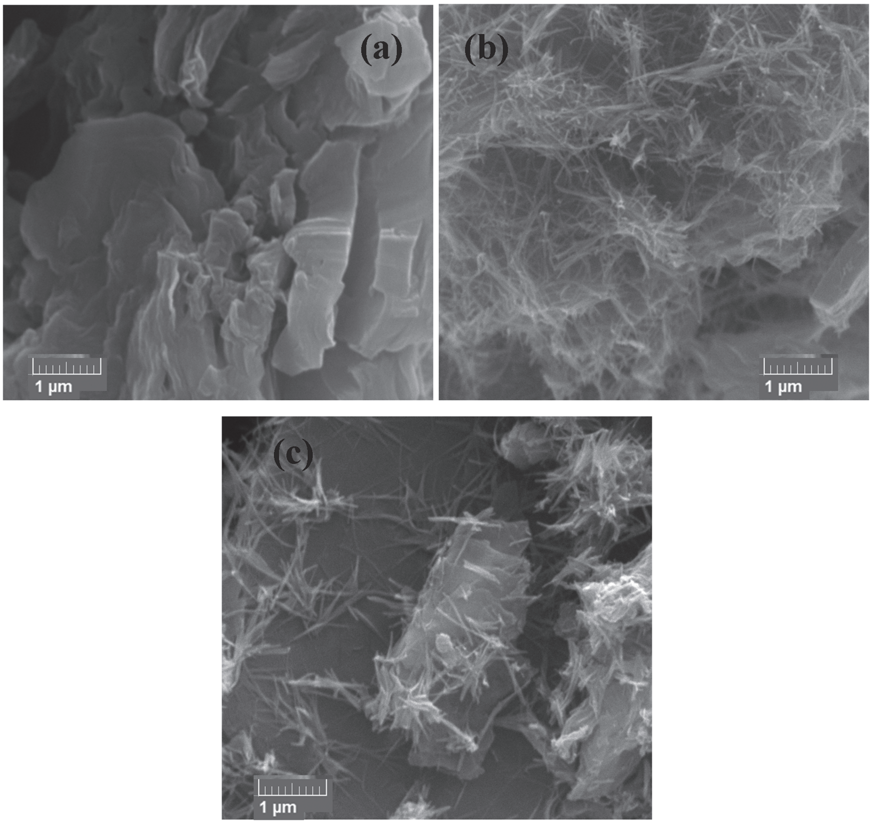

FIGURE 5 SEM images of (a) GO, (b) VO$(acac)_2$@en-GO, and (c) VO@Sal@en-GO

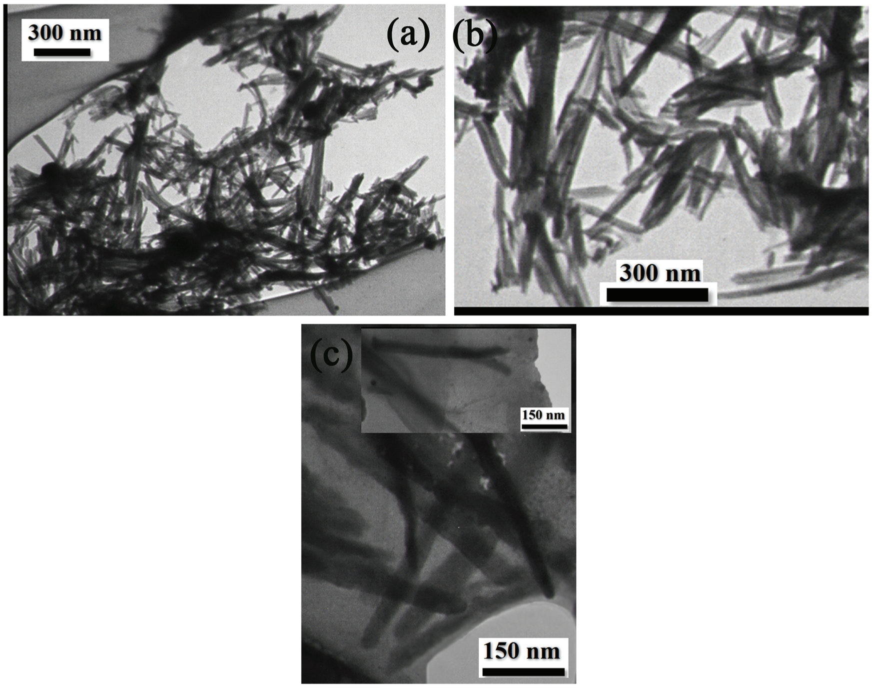

FIGURE 6 TEM images of (a) VO$(acac)_2$@en-GO and (b) VO@Sal@en-GO with two magnifications

isotherms with hysteresis loop at a relative pressure of $0.4 < p/p_0 < 1$. The surface areas of GO, en-GO, VO$(acac)_2$@en-GO, and VO@Sal@en-GO are 5.6392, 6.5234, 16.916, and 12.715 m^2/g, respectively. This increase of the surface area after complexation of vanadium complex on the GO surface is probably due to the new morphology formation on the surface of GO based on the SEM and TEM results (Figures 5 and 6). The obtained results are consistent with some reported articles.[46,47]

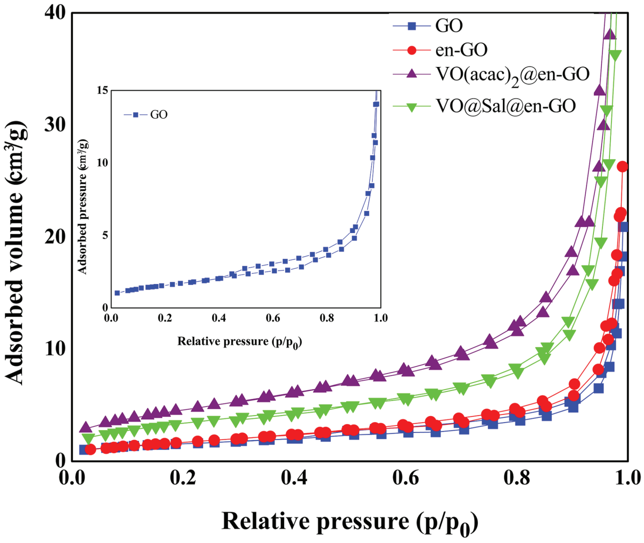

FIGURE 7 N_2 adsorption–desorption isotherms of GO, en-GO, VO(acac)$_2$@en-GO, and VO@Sal@en-GO

4 | CATALYTIC STUDIES

VO(acac)$_2$@en-GO and geraniol were used as models in order to find the optimum reaction conditions. For this purpose, various parameters such as the effect of catalyst amount, reaction time, and solvent were evaluated. It was found that whereas utilization of 10 mg of catalyst within 1, 1.5, and 2 h partially improved geraniol conversion (entries 1–3, Table 1), no increase in the conversion occurred by using 50 mg of the catalyst during the similar reaction times (entries 4–6, Table 1). Therefore, 10 mg of the catalyst was used within 2 h for other experiments.

The effect of solvent on the geraniol epoxidation is given in Table 2. As seen in this table, whereas oxidation reactions proceed effectively in acetonitrile, chloroform, and dichloromethane (entries 1–3, Table 2), they are rather sluggish in ethanol and methanol (entries 4–5, Table 2).

Having established the optimal reaction conditions, we examined the generality of this epoxidation on substrates such as geraniol, *trans*-2-hexen-1-ol, and 1-octen-3-ol in refluxing acetonitrile using 10 mg of catalyst (VO(acac)$_2$@en-GO and VO@Sal@en-GO) (Table 3). To avoid any overestimation of the catalytic activity of the systems under investigation, the catalytic activity (TON and TOF) of VO(acac)$_2$@en-GO and VO@Sal@en-GO has been calculated and included in Table 3. We have included the effect of the modified en-GO on the epoxidation (entry 7, Table 3) in order to make comparison with both (VO(acac)$_2$@en-GO and VO@Sal@en-GO) more convenient. Compared with the effect of en-GO which is totally ineffective as epoxidation catalyst for geraniol (entry 7, Table 3), the other two VO(acac)$_2$@en-GO and VO@Sal@en-GO exhibit catalytic activity for the conversion of geraniol to the corresponding epoxide with 97% and 88% yields, respectively (entries 1 and 4, Table 3). On the other hand, *trans*-2-hexen-1-ol and 1-octen-3-ol undergo epoxidation under the catalytic effect of (VO

TABLE 1 Conversion and selectivity of geraniol with different amounts of the VO(acac)$_2$@en-GO as catalyst at different reaction times[a]

Entry	Amounts of catalyst (mg)	Time (h)	Conversion (selectivity)%	TON	TOF (h^{-1})
1		1	94 (100)	323	323
2	10	1.5	96 (100)	330	220
3		2	97 (100)	334	167
4		1	89 (100)	61	61
5	50	1.5	94 (100)	65	43
6		2	94 (100)	65	32

[a] Reaction conditions: 10 and 50 mg catalyst, 10 mmol geraniol, 12 mmol TBHP, 5 mL CH_3CN. Entries 1–3 using 10 mg and entries 4–6 using 50 mg catalysts.

TABLE 2 Conversion and selectivity of geraniol with VO(acac)$_2$@en-GO as catalyst in different solvents[a]

Entry	Solvents	Conversion (selectivity)%	TON	TOF (h^{-1})
1	Acetonitrile	97 (100)	334	167
2	Chloroform	96 (100)	330	165
3	Dichloromethane	96 (100)	330	165
4	Ethanol	91 (100)	313	156
5	Methanol	87 (98)	299	150

[a] Reaction conditions: 10 mg catalyst, 10 mmol geraniol, 12 mmol TBHP, 5 mL solvent.

TABLE 3 Results obtained for catalyzed epoxidation of some allyl alcohols

Entry	Catalysts (mg)	Substrate	Conversion (selectivity)%	TON	TOF (h^{-1})
1	VO(acac)$_2$@en-GO	Geraniol[a]	97 (100)	334	167
2		*trans*-2-Hexen-1-ol[b]	74 (100)	51	17
3		1-Octen-3-ol[c]	36 (100)	25	2
4	VO@Sal@en-GO	Geraniol[a]	88 (100)	293	147
5		*trans*-2-Hexen-1-ol[b]	71 (100)	46	15
6		1-Octen-3-ol[c]	43 (75)	28	2
7	en-GO	Geraniol[a]	0	-	-

[a] Reaction conditions:10 mg catalyst, 10 mmol geraniol, 12 mmol TBHP, 5 ml CH_3CN, reflux for 2 h.

[b] Reaction conditions: 50 mg catalyst, 10 mmol *trans*-2-hexen-1-ol, 12 mmol TBHP, 5 ml CH_3CN, reflux for 3 h.

[c] Reaction conditions: 50 mg catalyst, 10 mmol 1-octen-3-ol, 12 mmol TBHP, 5 ml CH_3CN, reflux for 12 h.

(acac)$_2$@en-GO and VO@Sal@en-GO) although in a lesser extent than geraniol (entries 2–3 and 5–6, Table 3).

To make insight into the reaction mechanism, epoxidation of geraniol was carried out in the presence of diphenylamine as a radical scavenger.[48–50] Observation of no conversion inhibition indicated that reaction does not proceed through a radical mechanism. Therefore, it can be concluded that oxygen transfer from TBHP to allyl alcohols has proceeded via a concerted mechanism (Scheme 1). After the formation of Intermediates **I** and **II** via interaction of vanadium heterogeneous catalyst with TBHP and allyl alcohol, Intermediate **III** is generated through nucleophilic attack of the double bond to the electrophilic oxygen atom of the coordinated TBHP (Scheme 1). Subsequently, the epoxide resulted with elimination of *t*-BuOH and regeneration of catalyst. The decrease in conversion rates from geraniol to *trans*-2-hexen-1-ol and 1-octen-3-ol is an evidence in supporting the suggested mechanism because the formation rate of **III** depends on the number of alkyl substitutions present on the double bonds which in turn increase their nucleophilic character accordingly.[57] Recall that geraniol, *trans*-2-hexen-1-ol, and 1-octen-3-ol contain tri-, di-, and monosubstituted olefins, respectively.

To explore the reusability of the catalysts, it was separated at the end of reaction and reused in another reaction after washing several times with acetonitrile and drying. It was found that the conversion of geraniol epoxidation slightly dropped from 97% to 91% and 88 to 85% after using VO(acac)$_2$@en-GO and VO@Sal@en-GO in four runs, respectively (Figures 8 and 9).

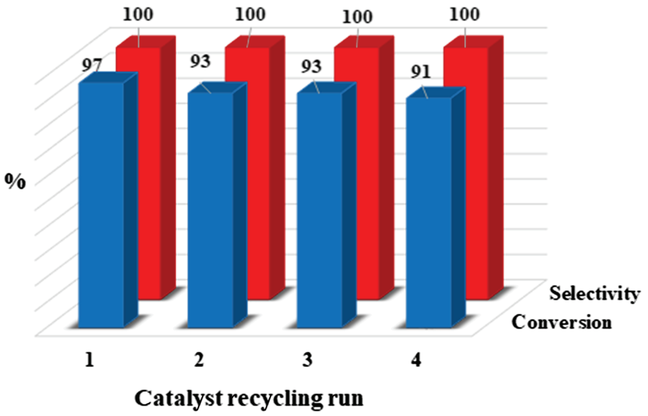

FIGURE 8 Effect of recycling of VO(acac)$_2$@en-GO on geraniol epoxidation

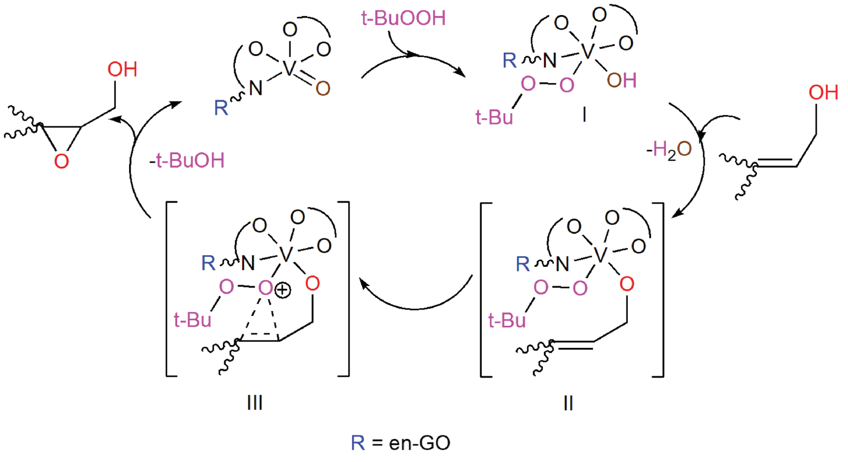

SCHEME 1 Suggested mechanism for the epoxidation of allyl alcohols catalyzed by VO(acac)$_2$@en-GO

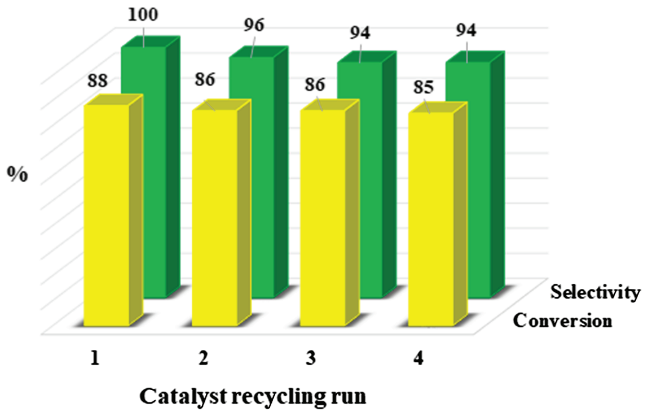

FIGURE 9 Effect of recycling of VO@Sal@en-GO on geraniol epoxidation

To further explore the stability of catalysts, the FT-IR spectra (Figures S1a,b and S3a,b) and XRD patterns (Figures S2a,b and S4a,b) of $VO(acac)_2$@en-GO and VO@Sal@en-GO) before and after using as catalyst on geraniol epoxidation were found to be similar (see Supporting Information). Such observations clearly indicate the stability and heterogeneity character of these catalysts. Moreover, because the filtrate did not show any activity toward epoxidation of geraniol, the obtained results confirmed the heterogeneous character of the catalyst. The vanadium percent for $VO(acac)_2$@en-GO before reaction was 14.82% and after reaction was 14.35%. The ICP determination for VO@Sal@en-GO before and after reaction was 15.76% and 14.95%, respectively.

4.1 | Comparison with other reported systems

The catalytic activity of geraniol epoxidation with $VO(acac)_2$@en-GO and VO@Sal@en-GO was compared with other reported catalysis systems (Table 4). It was found that the $VO(acac)_2$@en-GO with 97% conversion and 100% selectivity shows the most activity (TON and TOF) relative to the other catalysts.

5 | CONCLUSION

In conclusion, GO was initially modified with ethylenediamine (en) and designated as en-GO. Subsequently, $VO(acac)_2$ and the in situ generated VO@Salen

TABLE 4 Comparison of figure of merit of the present work (catalyst $VO(acac)_2$@en-GO and VO@Sal@en-GO) with other studies in the literature

Entry	Catalysts (mg)	Reaction conditions: amount of catalysts, solvent, temperature, time	Conversion (selectivity)%	TON/TOF (h^{-1})	Ref.
1	$VO(acac)_2$@en-GO[a]	10 mg, CH_3CN, reflux, 2 h	97 (100)	334/167	This work
2	VO@Sal@en-GO	10 mg, CH_3CN, reflux, 2 h	88 (100)	293/147	This work
3	CMK-3@[$VO(acac)_2$]	100 mg, CH_2Cl_2, RT, 2.5 h	100 (97)	100/91	[51]
4	CMK-3@APTES@[$VO(acac)_2$] with amine[b]	100 mg, CH_2Cl_2, RT, 2.5 h	98 (98)	74/68	[51]
5	[$VO(acac)_2$]APTES@SiO_2	100 mg, CH_2Cl_2, RT, 2 h	100 (99)	34/17	[52]
6	Fe_2O_3@SiO_2–NH_2–$VO(acac)_2$	50 mg, CH_2Cl_2, RT, 30 h	100 (96)	60/2	[53]
7	[$VO(acac)_2$]@APTES@laponite	100 mg, CH_2Cl_2, RT, 48 h	100 (97)	96/2	[54]
8	[$VO(acac)_2$]@APTES@K10	100 mg, CH_2Cl_2, RT, 48 h	100 (98)	96/2	[54]
9	[$VO(acac)_2$]@HMS[c]	100 mg, CH_2Cl_2, RT, 48 h	98 (98)	96/2	[55]
10	8-Quinolinol oxovanadium(IV) complex@graphene oxide	10 mg, CH_3CN, 70 °C, 8 h	83.7 (80)	199/25	[56]
11	Fe_3O_4@SiO_2@APTMS@[VO_2(bpca)][d]	50 mg, CH_3CN, reflux, 1 h	100 (100)	155/155	[57]
12	[$VO(acac)_2$]APTES@PCH[e]	100 mg, CH_2Cl_2, RT, 48 h	42 (81)	-	[58]
13	[$VO(acac)_2$]APTES@SBA-15	100 mg, CH_2Cl_2, RT, 48 h	34 (88)	-	[58]

[a] Reaction conditions:10 mg catalyst, 10 mmol geraniol, 12 mmol TBHP, 5 ml CH_3CN, reflux for 2 h.
[b] APTES, 3-aminopropyltriethoxysilane.
[c] HMS, hexagonal mesoporous silica.
[d] APTMS, 3-aminopropyltrimethoxysilane.
[e] PCH, porous clay heterostructure.

were immobilized onto the en-GO and designated as $VO(acac)_2$@en-GO and VO@Sal@en-GO, respectively. Characterization of the prepared catalysts was carried out with FT-IR, XRD, ICP, CHN, Raman, SEM, TEM, and BET techniques. The SEM images showed that nanofiber network and nanointerconnected needles have been formed after immobilization of vanadium compounds onto the modified en-GO. The prepared complex compounds were used as heterogeneous catalysts for epoxidation of some allyl alcohols such as geraniol, *trans*-2-hexene-1-ol, and 1-octen-3-ol. The epoxidation of geraniol with 97% conversion and 100% selectivity is considerable. Readily recycling of the catalyst and reusing for four successive catalytic runs without significant loss of activity revealed that this catalysis system deserves nomination for practical application.

ACKNOWLEDGMENTS

The authors appreciate Alzahra University for financial support.

AUTHOR CONTRIBUTIONS

Faezeh Farzaneh: Conceptualization; supervision. **zahra ahmadi:** Formal analysis; investigation; methodology. **zahra azarkamanzad:** Software. **Maryam Ghahremani:** Formal analysis.

CONFLICT OF INTEREST

There are no conflicts to declare.

DATA AVAILABILITY STATEMENT

Research data are not shared.

ORCID

Faezeh Farzaneh https://orcid.org/0000-0001-5651-8018
Zahra Ahmadi https://orcid.org/0000-0003-0139-354X
Zahra Azarkamanzad https://orcid.org/0000-0002-6115-2193

REFERENCES

[1] D. J. Cole-Hamilton, *Science* **2003**, *299*, 1702.
[2] T. J. Terry, T. D. P. Stack, *J. Am. Chem. Soc.* **2008**, *130*, 4945.
[3] D. T. Genna, A. G. Wong-Foy, A. J. Matzger, M. S. Sanford, *J. Am. Chem. Soc.* **2013**, *135*, 10586.
[4] Y. Yang, Y. Zhang, S. Hao, Q. Kan, *Cat. Com.* **2010**, *11*, 808.
[5] A. Bhaumik, T. Tatsumi, *J. Catal.* **2000**, *189*, 31.
[6] G. von Willingh, H. S. Abbo, S. J. Titinchi, *Catal. Today* **2014**, *227*, 96.
[7] L. Chen, Q. Xu, *Matter* **2019**, *1*, 57.
[8] Y. Fu, D. Sun, M. Qin, R. Huang, Z. Li, *RSC Adv.* **2012**, *2*, 3309.
[9] L. Hamidipour, F. Farzaneh, *C. R. Chim.* **2014**, *17*, 927.
[10] F. Farzaneh, Y. Sadeghi, *J. Mol. Catal. A: Chem.* **2015**, *398*, 275.
[11] D. Chen, H. Feng, J. Li, *Chem. Rev.* **2012**, *112*, 6027.
[12] D. Dodoo-Arhin, M. Fabiane, A. Bello, N. Manyala, *Ind. Eng. Chem. Res.* **2013**, *52*, 14160.
[13] R. C. Haddon, *Acc. Chem. Res.* **2013**, *46*, 2191.
[14] G. M. Scheuermann, L. Rumi, P. Steurer, W. Bannwarth, R. Mülhaupt, *J. Am. Chem. Soc.* **2009**, *131*, 8262.
[15] X. Chen, G. Wu, J. Chen, X. Chen, Z. Xie, X. Wang, *J. Am. Chem. Soc.* **2011**, *133*, 3693.
[16] Y. Yao, Z. Yang, H. Sun, S. Wang, *Ind. Eng. Chem. Res.* **2012**, *51*, 14958.
[17] Y. Liang, Y. Li, H. Wang, J. Zhou, J. Wang, T. Regier, H. Dai, *Nat. Mater.* **2011**, *10*, 780.
[18] W. Yu, L. Sisi, Y. Haiyana, L. Jiee, *RSC Adv.* **2020**, *10*, 15328.
[19] Q. Li, F. Fan, Y. Wang, W. Feng, P. Ji, *Ind. Eng. Chem. Res.* **2013**, *52*, 6343.
[20] V. Georgakilas, M. Otyepka, A. B. Bourlinos, V. Chandra, N. Kim, K. C. Kemp, P. Hobza, R. Zboril, K. S. Kim, *Chem. Rev.* **2012**, *112*, 6156.
[21] Y. Guo, C. Bao, L. Song, B. Yuan, Y. Hu, *Ind. Eng. Chem. Res.* **2011**, *50*, 7772.
[22] C. Su, K. P. Loh, *Acc. Chem. Res.* **2013**, *46*, 2275.
[23] H. Su, S. Wu, Z. Li, Q. Huo, J. Guan, Q. Kan, *Appl. Organomet. Chem.* **2015**, *29*, 462.
[24] Q. Yang, X. Pan, K. Clarke, K. Li, *Ind. Eng. Chem. Res.* **2012**, *51*, 310.
[25] M. Quintana, E. Vazquez, M. Prato, *Acc. Chem. Res.* **2013**, *46*, 138.
[26] J. U. Lee, W. Lee, J. W. Yi, S. S. Yoon, S. B. Lee, B. M. Jung, B. S. Kim, J. H. Byun, *J. Mater. Chem. A* **2013**, *1*, 12893.
[27] J. Zhang, Z. Xiong, X. Zhao, *J. Mater. Chem.* **2011**, *21*, 3634.
[28] Q. Zhao, C. Bai, W. Zhang, Y. Li, G. Zhang, F. Zhang, X. Fan, *Ind. Eng. Chem. Res.* **2014**, *53*, 4232.
[29] S. Mallakpour, A. Abdolmaleki, A. Karshenas, *Cat. Com.* **2017**, *92*, 109.
[30] G. Licini, V. Conte, A. Coletti, M. Mba, C. Zonta, *Coord. Chem. Rev.* **2011**, *255*, 2345.
[31] F. van de Velde, I. W. Arends, R. A. Sheldon, *J. Inorg. Biochem.* **2000**, *80*, 81.
[32] J. C. Pessoa, S. Etcheverry, D. Gambino, *Coord. Chem. Rev.* **2015**, *301*, 24.
[33] M. Sutradhar, L. M. Martins, M. F. C. G. da Silva, A. J. Pombeiro, *Coord. Chem. Rev.* **2015**, *301*, 200.
[34] W. S. Hummers Jr., R. E. Offeman, *J. Am. Chem. Soc.* **1958**, *80*.
[35] J. Zang, H. Qian, Z. Wei, Y. Cao, M. Zheng, Q. Dong, *Electrochim. Acta* **2014**, *118*, 112.
[36] D. Yuan, B. Wang, L. Wang, Y. Wang, Z. Zhou, *Compos. Part B Eng.* **2013**, *55*, 215.
[37] N. H. Kim, T. Kuila, J. H. Lee, *J. Mater. Chem. A* **2013**, *1*, 1349.
[38] E. Fedorova, V. Rybakov, V. Senyavin, A. Anisimov, L. Aslanov, *Crystallogr. Rep.* **2005**, *50*, 224.
[39] M. Acik, G. Lee, C. Mattevi, M. Chhowalla, K. Cho, Y. Chabal, *Nat. Mater.* **2010**, *9*, 840.
[40] D. Pan, S. Wang, B. Zhao, M. Wu, H. Zhang, Y. Wang, Z. Jiao, *Chem. Mater.* **2009**, *21*, 3136.
[41] S. M. El-Megharbel, R. Z. Hamza, M. S. Refat, *Spectrochim. Acta a* **2015**, *135*, 850.
[42] S. B. Gajera, J. V. Mehta, M. N. Patel, *RSC Adv.* **2015**, *5*, 21710.

[43] H. P. Mungse, S. Verma, N. Kumar, B. Sain, O. P. Khatri, *J. Mater. Chem.* **2012**, *22*, 5427.

[44] A. C. Ferrari, J. Meyer, V. Scardaci, C. Casiraghi, M. Lazzeri, F. Mauri, S. Piscanec, D. Jiang, K. Novoselov, S. Roth, *Phys. Rev. Lett.* **2006**, *97*, 187401.

[45] T. Wu, X. Wang, H. Qiu, J. Gao, W. Wang, Y. Liu, *J. Mater. Chem.* **2012**, *22*, 4772.

[46] S. Zhu, Y. Cen, M. Yang, J. Guo, C. Chen, J. Wang, W. Fan, *Appl. Catal. B-Environ.* **2017**, *211*, 89.

[47] Z. Li, S. Wu, D. Zheng, J. Liu, H. Liu, H. Lu, Q. Huo, J. Guan, Q. Kan, *Appl. Organomet. Chem.* **2014**, *28*, 317.

[48] L. M. Slaughter, J. P. Collman, T. A. Eberspacher, J. I. Brauman, *Inorg. Chem.* **2004**, *43*, 5198.

[49] F. Farzaneh, J. Taghavi, R. Malakooti, M. Ghandi, *J. Mol. Catal. A: Chem.* **2006**, *244*, 252.

[50] L. Hamidipour, F. Farzaneh, M. Ghandi, *React. Kinet. Mech. Cat.* **2012**, *107*, 421.

[51] S. Dorbes, C. Pereira, M. Andrade, D. Barros, A. Pereira, S. Rebelo, J. Araújo, J. Pires, A. Carvalho, C. Freire, *Micropor. Mesopor. Mat.* **2012**, *160*, 67.

[52] C. Pereira, J. F. Silva, A. M. Pereira, J. P. Arau'jo, G. Blanco, J. M. Pintado, C. Freire, *Catal. Sci. Technol.* **2011**, *1*, 784.

[53] C. Pereira, A. M. Pereira, P. Quaresma, P. B. Tavares, E. Pereira, J. P. Araújo, C. Freire, *Dalton T.* **2010**, *39*, 2842.

[54] C. Pereira, A. R. Silva, A. P. Carvalho, J. Pires, C. Freire, *J. Mol. Catal. A-Chem.* **2008**, *283*, 5.

[55] B. Jarrais, C. Pereira, A. R. Silva, A. P. Carvalho, J. Pires, C. Freire, *Polyhedron* **2009**, *28*, 994.

[56] Z. Li, S. Wu, D. Zheng, H. Liu, J. Hu, H. Su, J. Sun, X. Wang, Q. Huo, J. Guan, *Appl. Catal. A: General.* **2014**, *470*, 104.

[57] Z. Azarkamanzad, F. Farzaneh, M. Maghami, J. Simpson, M. Azarkish, *Appl. Organomet. Chem.* **2018**, *32*, e4168.

[58] C. Pereira, K. Biernacki, S. L. Rebelo, A. L. Magalhães, A. P. Carvalho, J. Pires, C. Freire, *J. Mol. Catal. A: Chem.* **2009**, *312*, 53.

SUPPORTING INFORMATION

Additional supporting information may be found online in the Supporting Information section at the end of this article.

How to cite this article: Farzaneh F, Ahmadi Z, Azarkamanzad Z, Ghahremani M. Immobilized some of vanadium compounds on modified graphene oxide as nanofiber network for epoxidation of allyl alcohols. *Appl Organomet Chem*. 2021;35:e6151. https://doi.org/10.1002/aoc.6151